Mechanism and Kinetics of Inducible Nitric Oxide Synthase Auto-*S*-Nitrosation and Inactivation

Brian C. Smith, Nathaniel B. Fernhoff, and Michael A. Marletta

SUPPORTING INFORMATION

Contents:

Supporting Experimental Procedures

Relative rates of GSNO and N-nitrosomorpholine reduction by GSH and TCEP. To 100 μM *S*-nitrosoglutathione (GSNO) or *N*-nitrosomorpholine was added 1 mM GSH or TCEP in 100 mM HEPES pH 7.5 in 600 μL total volume. Relative reduction rates were measured by the decrease in the maximum nitrosothiol absorbance at 344 nm for GSNO and the maximum *N*-nitrosamine absorbance at 343 nm for *N*-nitrosomorpholine.

Supporting Results

Reductants protect iNOS from S-nitrosation and inactivation. While NOS inactivation via *S*-nitrosation of the Zn^{2+}-tetrathiolate is most plausible, Rosenfeld *et al.* recently postulated the formation of N_5-nitrosated H_4B as an alternative inactivation mechanism (*1*). Therefore, the relative efficiency of *S*-nitrosothiol versus *N*-nitrosamine reduction by GSH and TCEP was determined (see Experimental Procedures). GSNO was used as a representative stable nitrosothiol. *N*-nitrosomorpholine was used as a mimic for N_5-nitrosated H_4B due to the structural similarity between these two molecules (Figure S2). While both GSH and TCEP are capable of reducing both *S*-nitrosothiols and *N*-nitrosamines, we found that TCEP is a highly potent and selective reducing agent for *S*-nitrosothiols over *N*-nitrosamines. In particular, TCEP reduction of GSNO was 850-fold faster than TCEP reduction of *N*-nitrosomorpholine. GSH is a comparatively weak reducing agent and only slightly more potent for *S*-nitrosothiols over *N*-nitrosamines. TCEP reduction of GSNO was 700-fold faster than GSH reduction of GSNO. GSH reduction of GSNO was only 5-fold faster than GSH reduction of *N*-nitrosomorpholine, although it should be noted that transnitrosation reactions between GSH and GSNO are silent in the absorbance assay used. The implications of these data on the primary mechanism of iNOS auto-inactivation are discussed below (see Supplementary Discussion).

Supporting Discussion

S-nitrosation is the major mechanism of iNOS auto-inactivation. While *S*-nitrosation in the only mechanism of NOS auto-inactivation consistent with all available data (see Discussion), H_4B nitrosation (*1*) and reaction with peroxynitrite (*2-5*) have also been postulated to result in NOS inactivation. However, several lines of evidence suggest that reaction with peroxynitrite is not a significant source of inactivation. While NOS is capable of forming peroxynitrite via radical recombination of NO and superoxide, peroxynitrite possesses an extremely short biological half-life of ~10 milliseconds, which results in steady-state concentrations of ~3 nM (*6*). However, previous *in vitro* studies required micromolar peroxynitrite concentrations to observe NOS inactivation, at least three orders of magnitude higher than physiological concentrations. Furthermore, a previous study that tested a variety of reactive oxygen/nitrogen species for nNOS inactivation found that only NO completely inactivated nNOS and that peroxynitrite was over two orders of magnitude less potent than NO towards nNOS inactivation (*7*). Additionally, we and others found that SOD, which decreases superoxide concentrations and therefore the ability to form peroxynitrite, failed to decrease NOS inactivation rates and in some cases resulted in a slight increase in inactivation rate (*7-10*). The slight increase in inactivation rates observed was presumably due to a slight increase in NO concentrations upon removal of the superoxide sink. Finally, under the saturating arginine and NADPH concentrations utilized in our assays the iNOS reductase and oxidase domains are well coupled and, while iNOS inactivation is observed, the generation of superoxide is expected to be negligible. Taken together, these results suggest that reaction with peroxynitrite is not a significant source of NOS inactivation.

Rosenfeld *et al.* recently reported that H_4B bound to iNOS displayed increased electron density when crystallized in the presence of 50 mM Cys-SNO and postulated the formation of N_5-nitrosated H_4B (*1*). This concentration of Cys-SNO is approximately five orders of magnitude higher than physiological Cys-SNO concentrations (*11*). The authors proposed that formation of N_5-nitrosated H_4B is a potential mechanism of NOS auto-inactivation, which would occur through radical recombination of the NO radical and the N_5-centered H_4B radical. However, as release of the NO radical is coupled to

reduction of the tetrahydrobiopterin radical (*12*), the two radicals are not predicted to coexist during turnover.

To kinetically distinguish between iNOS auto-inactivation by *S*-nitrosation or formation of N_5-nitrosated H_4B, we compared the ability of two reductants with distinct reduction mechanisms, GSH and TCEP, to protect against iNOS auto-inactivation as well as reduce *S*-nitrosothiols and *N*-nitrosamines. TCEP is a potent and selective reducing agent for *S*-nitrosothiols over *N*-nitrosamines, whereas GSH is a weaker reducing agent and only a slightly more potent reducing agent for nitrosothiols compared to *N*-nitrosamines (see Supporting Results). The efficiency of TCEP prevention of iNOS inactivation ($k_{10}^{TCEP}/K_{m,\,app}^{TCEP}$) was ~200-fold higher than the corresponding efficiency with GSH. As TCEP is not predicted to possess an iNOS binding site, this increase in efficiency of TCEP compared to GSH is best attributed to an increased ability to reduce the *S*-nitrosated Zn^{2+}-tetrathiolate. If N_5-nitrosated H_4B were a significant source of iNOS auto-inactivation, then a much smaller difference in efficiencies between TCEP and GSH would be expected as TCEP reduction of *N*-nitrosomorpholine was only ~4-fold faster than GSH reduction of *N*-nitrosomorpholine. A previous study showed that ascorbate (10 mM) and GSH (7 mM) were equally capable of protecting nNOS from inactivation (*10*). As ascorbate selectively reduces nitrosothiols over other oxidized cysteines (the basis of the biotin switch method (*13*)), this further suggests that the protective effect of GSH and TCEP is through reduction of the *S*-nitrosated NOS. We were unable to utilize ascorbate here as it interfered with the MbO_2 assay. Furthermore, iNOS inactivation was irreversible consistent with irreversible dimer dissociation following *S*-nitrosation. This irreversible inactivation was inconsistent with inactivation by H_4B nitrosation as, based on the crystal structure (*1*), N_5-nitrosated H_4B remains bound and the iNOS dimer remains intact, indicating that GSH addition following iNOS inactivation should recover iNOS activity if N_5-nitrosated H_4B were the source of inactivation. Finally, as nitrosamines are significantly more stable than nitrosothiols, GSH reversal of H_4B nitrosation to form GSNO would be energetically unfavorable whereas GSNO formation from reaction of GSH with a nitrosothiol is energetically neutral. Indeed, we

did not observe the peak absorbance characteristic of GSNO (λ_{max} = 334 nm) when GSH was mixed with the N_5-nitrosated H_4B analog *N*-nitrosomorpholine; only a decrease in the peak *N*-nitrosomorpholine absorbance (λ_{max} = 343 nm) was observed indicating that GSNO was not formed in significant amounts (data not shown). Taken together, we conclude that H_4B nitrosation or reaction with peroxynitrite does not significantly contribute to iNOS auto-inactivation and that iNOS *S*-nitrosation is the major mechanism of inactivation.

Transnitrosation between iNOS and GSH. While GSH is clearly capable of lowering NOS *S*-nitrosation (Figure 5), GSH likely does not possess a specific binding site within NOS. In a previous study, nNOS did not bind GSH-agarose arguing against a specific GSH binding site (*36*). Another previous study did observe some evidence for GSH binding to the iNOS oxidase domain by saturation transfer difference NMR spectroscopy, but the potential binding site was not elucidated (*70*). Here, protection of iNOS auto-inactivation by TCEP and GSH correlated with their relative reducing strength, not their ability to bind iNOS (Figure 4). TCEP and GSH are structurally divergent and TCEP unlikely to bind iNOS. However, TCEP was significantly more potent than GSH in protection from iNOS auto-inactivation. While we did observe saturation kinetics for GSH protection from iNOS auto-inactivation, the apparent K_m value for this effect was 13 mM (Table 1). Therefore, it appears likely that GSH reacts with *S*-nitrosated iNOS in a manner similar to a Theorell-Chance kinetic mechanism (*71*, *72*) in which no complex is formed prior to reaction but saturation kinetics are observed.

References

1. Rosenfeld, R. J., Bonaventura, J., Szymczyna, B. R., Maccoss, M. J., Arvai, A. S., Yates, J. R., Tainer, J. A., and Getzoff, E. D. (2010) Nitric-oxide Synthase Forms N-NO-pterin and S-NO-Cys: Implications for activity, allostery, and regulation, *J Biol Chem 285*, 31581–31589.
2. Chen, W., Druhan, L. J., Chen, C.-A., Hemann, C., Chen, Y.-R., Berka, V., Tsai, A.-L., and Zweier, J. L. (2010) Peroxynitrite induces destruction of the tetrahydrobiopterin and heme in endothelial nitric oxide synthase: transition from reversible to irreversible enzyme inhibition, *Biochemistry 49*, 3129–3137.
3. Zou, M.-H., Shi, C., and Cohen, R. A. (2002) Oxidation of the zinc-thiolate complex and uncoupling of endothelial nitric oxide synthase by peroxynitrite, *J. Clin. Invest. 109*, 817–826.
4. Hühmer, A. F. R., Nishida, C. R., Ortiz de Montellano, P. R., and Schöneich, C. (1997) Inactivation of the Inducible Nitric Oxide Synthase by Peroxynitrite, *Chemical research in toxicology*. American Chemical Society *10*, 618–626.
5. Pasquet, J. P., Zou, M. H., and Ullrich, V. (1996) Peroxynitrite inhibition of nitric oxide synthases, *Biochimie 78*, 785–791.
6. Ferrer-Sueta, G., and Radi, R. (2009) Chemical biology of peroxynitrite: kinetics, diffusion, and radicals, *ACS Chem Biol 4*, 161–177.
7. Kotsonis, P., Frey, A., Fröhlich, L. G., Hofmann, H., Reif, A., Wink, D. A., Feelisch, M., and Schmidt, H. H. (1999) Autoinhibition of neuronal nitric oxide synthase: distinct effects of reactive nitrogen and oxygen species on enzyme activity, *Biochem J 340 (Pt 3)*, 745–752.
8. Buga, G. M., Griscavage, J. M., Rogers, N. E., and Ignarro, L. J. (1993) Negative feedback regulation of endothelial cell function by nitric oxide, *Circ Res 73*, 808–812.
9. Griscavage, J. M., Rogers, N. E., Sherman, M. P., and Ignarro, L. J. (1993) Inducible nitric oxide synthase from a rat alveolar macrophage cell line is inhibited by nitric oxide, *J Immunol 151*, 6329–6337.
10. Hofmann, H., and Schmidt, H. H. (1995) Thiol dependence of nitric oxide synthase, *Biochemistry 34*, 13443–13452.
11. Giustarini, D., Milzani, A., Dalle-Donne, I., and Rossi, R. (2007) Detection of S-nitrosothiols in biological fluids: A comparison among the most widely applied methodologies, *Journal of Chromatography B 851*, 124–139.
12. Woodward, J. J., Nejatyjahromy, Y., Britt, R. D., and Marletta, M. A. (2010) Pterin-centered radical as a mechanistic probe of the second step of nitric oxide synthase, *J Am Chem Soc 132*, 5105–5113.
13. Jaffrey, S. R., and Snyder, S. H. (2001) The biotin switch method for the detection of S-nitrosylated proteins, *Sci STKE 86*, pl1–9.
14. Rosenfeld, R. J., Garcin, E. D., Panda, K., Andersson, G., Aberg, A., Wallace, A. V., Morris, G. M., Olson, A. J., Stuehr, D. J., Tainer, J. A., and Getzoff, E. D. (2002) Conformational changes in nitric oxide synthases induced by chlorzoxazone and nitroindazoles: crystallographic and computational analyses of inhibitor potency, *Biochemistry 41*, 13915–13925.
15. Theorell, H., and Chance, B. (1951) Studies on liver alcohol dehydrogenase. 2. The kinetics of the compound of horse liver alcohol dehydrogenase and reduced diphosphopyridine nucleotide, *Acta Chem. Scand. 5*, 1127–1144.
16. Segel, I. H. (1975) Enzyme Kinetics. John Wiley & Sons, New York.

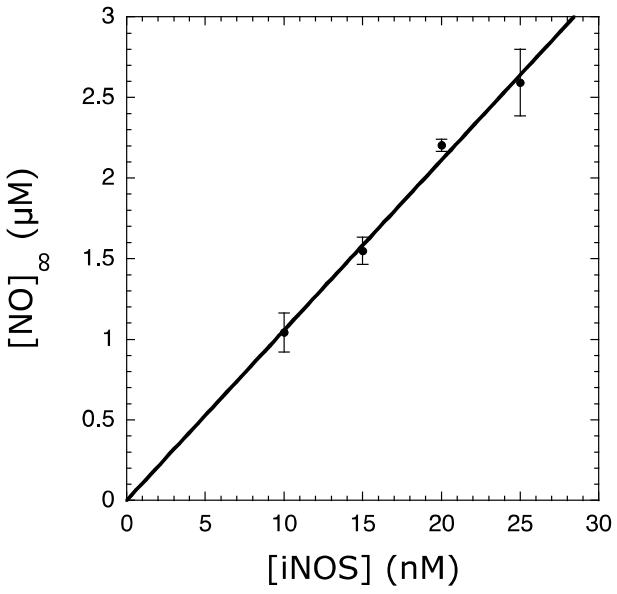

Figure S1. Plot of $[NO]_\infty$ versus iNOS concentration. Reactions contained varying concentrations of iNOS, 5 mM Arg, 200 μM NADPH, 50 mM NaCl, 4 μM MbO_2, and 100 mM HEPES pH 7.5 in 300 μL total volumes in a 96-well microplate. NO formation was determined by the increase in absorbance at 401 nm observed upon reaction of NO with MbO_2 to form metMb and nitrite. The concentration of NO formed at infinite time ($[NO]_\infty$) was determined through fitting progress curves of NO formation to equation 3 using non-linear regression in Kaleidagraph (Synergy Software; Reading, PA). The plot of of $[NO]_\infty$ versus iNOS concentration was fitted to a straight line using linear regression.

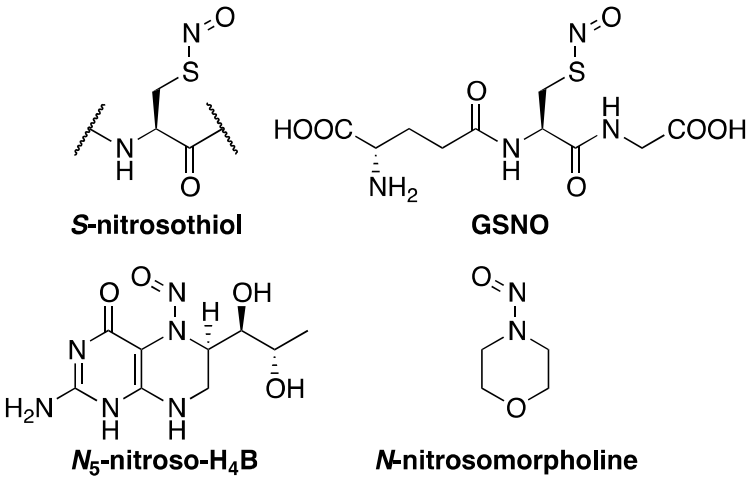

Figure S2. Chemical structures of a protein nitrosothiol, GSNO, N_5-nitrosated H_4B, and *N*-nitrosomorpholine.

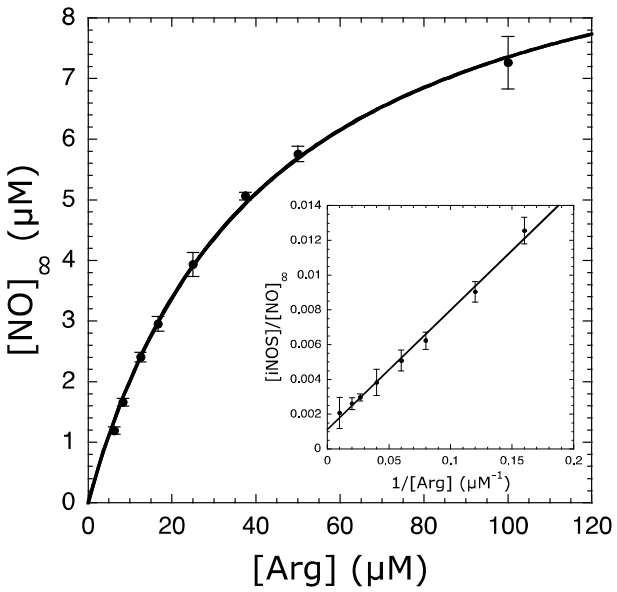

Figure S3. Plot of $[NO]_\infty$ versus Arg concentration. Individual reactions contained 15 nM iNOS, 6.25 to 100 μM Arg, 200 μM NADPH, 50 mM NaCl, 8 μM MbO_2, and 100 mM HEPES pH 7.5 in 300 μL total volumes in a 96-well microplate. NO formation was measured via the change in absorbance at 401 nm upon reaction of oxyMb with NO. The plot of $[NO]_\infty$ versus Arg concentration was fitted to equation 9 using non-linear regression in Kaleidagraph (Synergy Software; Reading, PA). The plot of $[iNOS]/[NO]_\infty$ versus 1/[Arg] (inset) was fitted to equation 10 using least-squares linear regression.